



HAL
open science

Structural and Functional Characterization of VanG d-Ala:d-Ser Ligase Associated with Vancomycin Resistance in *Enterococcus faecalis*

Djalal Meziane-Cherif, Frederick A. Saul, Ahmed Haouz, Patrice Courvalin

► **To cite this version:**

Djalal Meziane-Cherif, Frederick A. Saul, Ahmed Haouz, Patrice Courvalin. Structural and Functional Characterization of VanG d-Ala:d-Ser Ligase Associated with Vancomycin Resistance in *Enterococcus faecalis*. *Journal of Biological Chemistry*, 2012, 287 (45), pp.37583 - 37592. 10.1074/jbc.m112.405522 . pasteur-03525398

HAL Id: pasteur-03525398

<https://pasteur.hal.science/pasteur-03525398>

Submitted on 13 Jan 2022

HAL is a multi-disciplinary open access archive for the deposit and dissemination of scientific research documents, whether they are published or not. The documents may come from teaching and research institutions in France or abroad, or from public or private research centers.

L'archive ouverte pluridisciplinaire **HAL**, est destinée au dépôt et à la diffusion de documents scientifiques de niveau recherche, publiés ou non, émanant des établissements d'enseignement et de recherche français ou étrangers, des laboratoires publics ou privés.



Distributed under a Creative Commons Attribution 4.0 International License

Structural and Functional Characterization of VanG D-Ala:D-Ser Ligase Associated with Vancomycin Resistance in *Enterococcus faecalis**

Received for publication, July 27, 2012, and in revised form, September 6, 2012. Published, JBC Papers in Press, September 11, 2012, DOI 10.1074/jbc.M112.405522

Djalal Meziane-Cherif^{†1}, Frederick A. Saul[§], Ahmed Haouz[§], and Patrice Courvalin[‡]

From the Institut Pasteur, [‡]Unité des Agents Antibactériens and [§]Plate-forme 6, CNRS-UMR3528, 25 rue du Dr. Roux, 75724 Paris Cedex 15, France

Background: D-Ala:D-Lac and D-Ala:D-Ser ligases are key enzymes in vancomycin resistance.

Results: The VanG D-Ala:D-Ser ligase structure provided insight into its molecular specificity and allowed the selection of a specific peptide inhibitor.

Conclusion: D-Ala:D-Lac and D-Ala:D-Ser ligases share specific determinants.

Significance: This study sheds light on the molecular specificity and evolution of D-Ala:D-X ligases and could help in designing inhibitors to overcome vancomycin resistance.

D-Alanyl:D-lactate (D-Ala:D-Lac) and D-alanyl:D-serine ligases are key enzymes in vancomycin resistance of Gram-positive cocci. They catalyze a critical step in the synthesis of modified peptidoglycan precursors that are low binding affinity targets for vancomycin. The structure of the D-Ala:D-Lac ligase VanA led to the understanding of the molecular basis for its specificity, but that of D-Ala:D-Ser ligases had not been determined. We have investigated the enzymatic kinetics of the D-Ala:D-Ser ligase VanG from *Enterococcus faecalis* and solved its crystal structure in complex with ADP. The overall structure of VanG is similar to that of VanA but has significant differences mainly in the N-terminal and central domains. Based on reported mutagenesis data and comparison of the VanG and VanA structures, we show that residues Asp-243, Phe-252, and Arg-324 are molecular determinants for D-Ser selectivity. These residues are conserved in both enzymes and explain why VanA also displays D-Ala:D-Ser ligase activity, albeit with low catalytic efficiency in comparison with VanG. These observations suggest that D-Ala:D-Lac and D-Ala:D-Ser enzymes have evolved from a common ancestral D-Ala:D-X ligase. The crystal structure of VanG showed an unusual interaction between two dimers involving residues of the omega loop that are deeply anchored in the active site. We constructed an octapeptide mimicking the omega loop and found that it selectively inhibits VanG and VanA but not *Staphylococcus aureus* D-Ala:D-Ala ligase. This study provides additional insight into the molecular evolution of D-Ala:D-X ligases and could contribute to the development of new structure-based inhibitors of vancomycin resistance enzymes.

are a serious public health threat in hospitals worldwide. Their increased prevalence and their ability to transfer vancomycin resistance to other bacterial species, including methicillin-resistant *Staphylococcus aureus*, have made them a challenging nosocomial pathogen (1).

The mechanism of action of glycopeptides is the inhibition of extracellular steps during peptidoglycan synthesis (2). These antibiotics interact with the D-Ala-D-Ala terminus of the uncross-linked peptidoglycan pentapeptide (N-acetyl-muramyl-L-Ala-D-Glu-Lys-D-Ala-D-Ala). This interaction involves five hydrogen bonds that sequester the D-Ala-D-Ala dipeptide, thereby inhibiting the activity of the transpeptidases necessary for cell wall cross-linking (3). Resistance results from the production of modified peptidoglycan precursors ending in D-Ala-D-Lac² (VanA-, VanB-, VanD-, and VanM-type) or D-Ala-D-Ser (VanC-, VanE-, VanG-, VanL, and VanN-type) (4–6). This modification results in the loss of a hydrogen bond in the complex between D-Ala-D-Lac and vancomycin and to hydroxyl-mediated steric hindrance with D-Ala-D-Ser. As a consequence, vancomycin exhibits, respectively, a 1000- and 6-fold decrease in binding affinity (7, 8). In VanA-, VanB-, VanD-, or VanM-type enterococci, synthesis of D-Ala-D-Lac requires the presence of an ATP-dependent ligase (VanA, VanB, VanD, or VanM) of altered specificity when compared with the host D-Ala:D-Ala ligase (Ddl) (4, 9). In VanC-, VanE-, VanG-, VanL-, and VanN-type strains, the ligase genes encode proteins that catalyze the synthesis of D-Ala-D-Ser (8, 10). These enzymes act at a critical step in reprogramming the peptidoglycan biosynthetic pathway and are therefore important targets for developing new antibiotics. The enzymatic reaction is a two-step process, with the transfer of the γ -phosphoryl of ATP to the carboxyl group of the first D-Ala leading to an acylphosphate intermediate and ADP. The acyl carbon atom of the acylphosphate then reacts with the amino group of the second D-Ala to yield a tetrahedral intermediate that dissociates to produce

The glycopeptide antibiotics vancomycin and teicoplanin are important for the treatment of serious infections caused by Gram-positive cocci. *Enterococcus* spp. resistant to vancomycin

* This article was selected as a Paper of the Week.

The atomic coordinates and structure factors (code 4FU0) have been deposited in the Protein Data Bank (<http://www.pdb.org/>).

¹ To whom correspondence should be addressed. Tel.: 33-1-44-38-94-24; Fax: 33-1-45-68-83-19; E-mail: djalal.meziane-cherif@pasteur.fr.

² The abbreviations used are: D-Lac, D-lactate; Ddl, D-Ala:D-Ala ligase; LmDdl2, Ddl from *L. mesenteroides*; StaDdl, Ddl from *S. aureus*.

Molecular Specificity of D-Ala:D-Ser Ligases

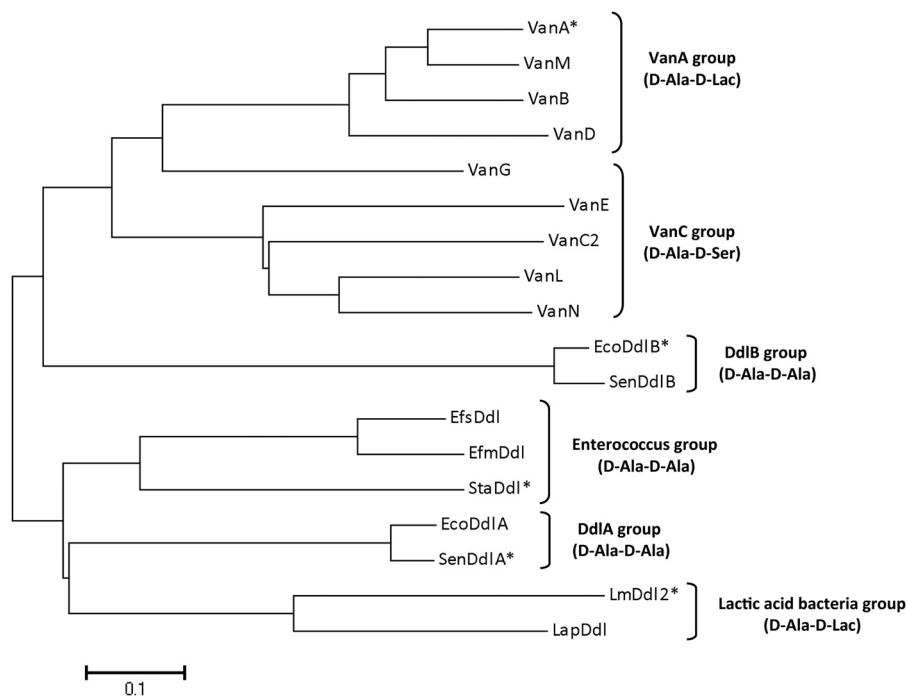


FIGURE 1. **Molecular phylogenetic analysis using the neighbor-joining method (38) of 18 amino acid sequences of representative D-Ala:D-X ligases from different species.** The ligases listed are: VanA (*E. faecium*, AAA65956); VanB (*Enterococcus faecalis*, Q06893); VanD (*E. faecium*, AAM09849); VanM (*E. faecium*, ACL82961); VanG (*E. faecalis*, AAQ16273); VanC2 (*Enterococcus casseliflavus*, AAA60990); VanE (*E. faecalis*, ABA71731); VanL (*E. faecalis*, ABX54687); VanN (*E. faecium*, AEP40500); EcoDdlB (*E. coli*, EGT67290); SenDdlA (*Salmonella enterica typhimurium*, 3Q1K_D); SenDdlB (*S. enterica*, CAD01287); EfsDdl (*E. faecalis*, ZP_05595436); EfmDdl (*E. faecium*, ZP_00604712); StaDdl (*S. aureus*, ADL66141); EcoDdlA (*E. coli*, NP_286119); LmDdl2 (*L. mesenteroides*, AET29676); LapDdl (*Lactobacillus plantarum*, NP_785815). Asterisks indicate ligases for which the crystal structure is available. Alignment was performed using the program ClustalW. Evolutionary analyses were conducted using MEGA5 (39). The scale bar at the bottom indicates the branch length.

phosphate and D-Ala-D-Ala. Kinetic studies have identified two subsites for D-Ala binding in the active site (11, 12). Structural (13–18) and mutagenesis (19) studies have shown that many of the residues involved in substrate binding and catalysis are conserved in the D-Ala:D-X ligase superfamily.

The D-Ala:D-X ligase superfamily can be divided into six families based on sequence homology (Fig. 1). Three are D-Ala:D-Ala ligases, two are D-Ala:D-Lac ligases, and one is a D-Ala:D-Ser ligase (20). VanG is a singular example because it is associated with a D-Ala-D-Ser mechanism of resistance, whereas it is phylogenetically closer to the VanA group. An intriguing question in vancomycin resistance is the molecular evolution of the D-Ala:D-Ala ligases that led to a switch in substrate specificity and thus to the reprogramming of peptidoglycan synthesis. Because the first reaction step is common to all D-Ala:D-X ligases, specificity for the second substrate must be attributed to differences in the second binding site (subsite 2). D-Ala:D-Lac ligase specificity was previously studied by the structure determination of VanA (14) and of the naturally resistant LmDdl2 from *Leuconostoc mesenteroides* (16). Both structures were determined in complex with a phosphinophosphate inhibitor, which is a close analog of a tetrahedral intermediate in the catalytic reaction. The basis for D-Ala:D-Ser ligase specificity is not fully understood due, in part, to the absence of three-dimensional structures for this family of enzymes. Previous studies of the VanC2 D-Ala:D-Ser ligase suggested that residues Arg-322 and Phe-250 corresponding to, respectively, Arg-324 and Phe-252 in VanG could be responsible for the greater affinity of the second binding site for D-Ser (21). However, the role of these

residues in controlling substrate specificity has not been elucidated. To gain insight into the molecular specificity of D-Ala:D-Ser ligases, we have studied the function and crystal structure of VanG and provide evidence that the triad Asp-243, Phe-252, and Arg-324 is the molecular signature for D-Ala-D-Ser specificity.

EXPERIMENTAL PROCEDURES

Cloning, Protein Expression, and Purification—Production and purification of VanG have been reported previously (22). Briefly, VanG engineered to have a C-terminal His tag was produced from *Escherichia coli* BL21(DE3)-pREP4 harboring plasmid pAT911 [pET28a(+) Ω vanG]. The protein was purified by nickel-affinity chromatography and Superdex 75 gel filtration to yield 30–40 mg from a 1-liter culture. VanA and the D-Ala:D-Ala ligase from *S. aureus* (StaDdl) were produced and purified from *E. coli* BL21(DE3)-pREP4 harboring, respectively, plasmids pIADL54 [pET28b(+) Ω vanA] and pAT518 [pET28a(+) Ω staddl] as described (23, 24).

Substrate Specificity and Kinetic Analysis—Substrate specificity was assayed by thin-layer chromatographic (TLC) analysis of radioactive dipeptides produced by VanG (20 μ g) following incubation of D-[1- 14 C]Ala or D-[1- 14 C]Ser (5 mM) with 80 mM of additional amino acid or hydroxy acid (25). The D-Ala:D-Lac ligase activity was studied by incubation of D-Ala (5 mM) with 80 mM D-[1- 14 C]Lac. Kinetic parameters of D-Ala:D-X ligase activities were determined using the ADP release spectrophotometric assay previously described (26). The assay mixture contained 100 mM Hepes (pH 7.5), 10 mM KCl, 10 mM

MgCl₂, 10 mM ATP, 2.5 mM phosphoenolpyruvate, 0.2 mM NADH, 50 units/ml pyruvate kinase/L-lactate dehydrogenase, and substrate at increasing concentrations. Kinetic constants (the mean values of at least three independent measurements) were obtained by fitting experimental data to the equations described by Neuhaus (11) using the program EnzFitter (BIOSOFT, Cambridge, UK). K_m for ATP was measured at a fixed 80 mM concentration of D-Ala.

Inhibition by Peptide Omega-1—Peptide Omega-1 (formyl-DYTEKYTL-NH₂) was obtained from Peptide 2.0 Inc. (Chantilly, VA). Inhibition of VanG, VanA, and StaDdl was assayed against D-Ala-D-Ala formation by the ADP release spectrophotometric assay (26). The assay mixture was the same as above with the addition of 5% v/v of dimethyl sulfoxide (DMSO) for peptide solubilization. The IC₅₀ values were similarly determined by nonlinear regression analysis using EnzFitter.

Structure Determination—Crystallization, data collection, and structure determination of the VanG-ADP complex were reported previously (22). Briefly, crystals were obtained with the hanging-drop vapor diffusion method by mixing 2 μl of protein solution at 14.5 mg/ml containing 10 mM ADP with 2 μl of crystallization solution containing 0.5 M ammonium sulfate, 0.9 M lithium sulfate, and 0.1 M sodium citrate, pH 5.6, and equilibrated against 1 ml of reservoir solution. The best crystal

was flash-cooled in liquid nitrogen using the crystallization solution containing 25% (v/v) of glycerol as a cryoprotectant, and x-ray diffraction data were collected on beamline Proxima 1 at the SOLEIL synchrotron (St. Aubin, France). The crystallographic parameters and data statistics were reported (22); the protein crystallized in space group P3₁21 ($a = b = 116.1$ Å, $c = 177.2$ Å) with two independent molecules forming a dimer in the asymmetric unit, and diffraction data extended to 2.35 Å resolution. The structure was determined by molecular replacement with the program Phaser (27) using coordinates of the VanA D-Ala:D-Lac ligase from *Enterococcus faecium* (Protein Data Bank (PDB) code 1E4E) (14), which has 45% sequence identity with VanG. The structure was refined by alternate cycles of restrained maximum likelihood refinement using the program Refmac5 (28) as implemented in the CCP4 program suite (29). Manual adjustments to the model were made with Coot (30). The final refinement statistics and model parameters are shown in Table 1. All structural representations were generated with PyMOL (31).

RESULTS

Substrate Specificity of VanG—Thin layer chromatographic assay showed that similarly to VanA (25) and VanC2 (32), VanG was able to synthesize several mixed dipeptides (Fig. 2). Using D-[1-¹⁴C]Ala and D-X (amino acid or hydroxy acid), VanG synthesized simultaneously D-Ala-D-X and D-Ala-D-Ala. However, in the presence of D-Ser, D-Ala-D-Ala was not detected, suggesting that VanG exhibits a high specificity for D-Ser at subsite 2 (Fig. 2A). D-Threonine was also a good substrate as judged by the low amount of D-Ala-D-Ala formed. Alternatively, VanG could also accommodate a number of amino acids such as D-aminobutyrate, D-norvaline, D-norleucine, D-methionine, and to a lesser extent, D-valine, D-leucine, and D-isoleucine. Aromatic amino acids such as D-phenylalanine and D-tryptophan were poor substrates, arguing that subsite 2 could be a relatively small cavity unable to accommodate β-branched and bulky amino acid side chains. VanG did not synthesize D-Ala-D-Lac or D-Ala-D-hydroxyvalerate as confirmed by using D-[¹⁴C]lactate and D-Ala in the assay mixture (data not shown).

TABLE 1
Refinement statistics and model parameters

Values in parentheses are for the highest resolution shell.

Resolution (Å)	33.5–2.35 (2.38–2.35)
R-value (working set)	0.190 (0.328)
R _{free}	0.224 (0.404)
No. of reflections	55,248 (2050)
Non-hydrogen atoms	5747
Amino acid residues	686
Water molecules	300
r.m.s. ^a deviations from ideality	
Bond lengths (Å)	0.013
Bond angles (°)	1.402
Mean protein B factor (Å ²)	43.03
Ramachandran statistics	
Most favored regions	91.9%
Additional allowed regions	8.1%

^a r.m.s., root mean square.

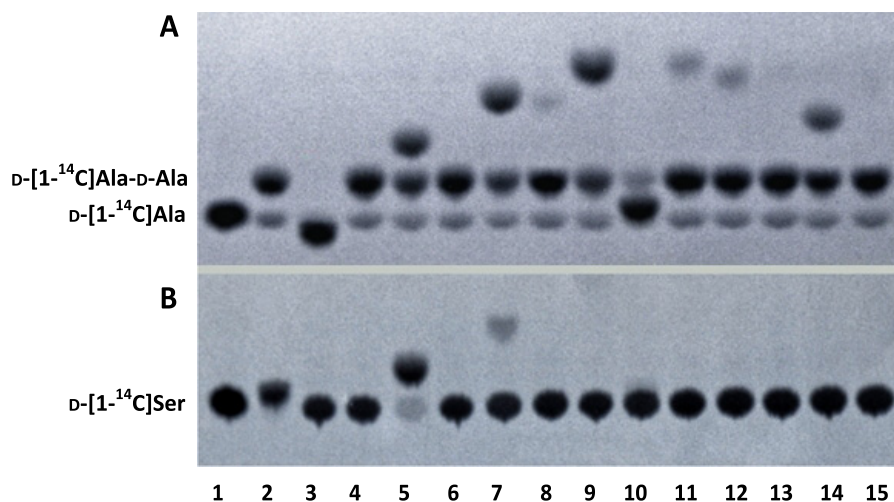


FIGURE 2. Substrate specificity of VanG as D-Ala:D-X ligase (A) and D-Ser:D-X ligase (B) tested by TLC. Lane 1, no enzyme; lane 2, D-alanine; lane 3, D-serine; lane 4, D-lactate; lane 5, D,L-aminobutyrate; lane 6, D,L-hydroxyvalerate; lane 7, D-norvaline; lane 8, D-valine; lane 9, D-norleucine; lane 10, D-threonine; lane 11, D-leucine; lane 12, D-phenylalanine; lane 13, D-isoleucine; lane 14, D-methionine; lane 15, D-tryptophan.

Molecular Specificity of D-Ala:D-Ser Ligases

TABLE 2

Kinetic parameters of VanG, VanA, and VanC2 D-Ala:D-X ligases

ND, not detected; NA, not applicable; Abu, 2-aminobutyric acid; —, not determined.

Product/ Substrate	VanG enzyme				VanA enzyme				VanC2 enzyme ^a			
	K_{m1}	K_{m2}	k_{cat}	k_{cat}/K_{m2}	K_{m1}	K_{m2}	k_{cat}	k_{cat}/K_{m2}	K_{m1}	K_{m2}	k_{cat}	k_{cat}/K_{m2}
D-Ala-D-Ala	0.4 ± 0.17	32.7 ± 9.5	7.8 ± 0.6	0.24 ± 0.03	1.4 ± 0.3	215 ± 62	9.5 ± 1.1	0.04 ± 0.002	—	—	—	—
D-Ala-D-Lac	—	—	ND	—	—	1.1 ± 0.3	3.4 ± 1.0	3.1 ± 0.1	—	—	—	—
D-Ala-D-Ser	—	0.22 ± 0.01	5.5 ± 0.2	24.8 ± 0.16	—	54.6 ± 6.5	3.0 ± 1.2	0.05 ± 0.01	—	1.8	8.16	4.5
D-Ser-D-Ser	1.8 ± 0.9	16.3 ± 2.6	6.1 ± 1.4	0.37 ± 0.05	—	—	—	—	—	—	ND	—
D-Ala-D-Abu	—	4.5 ± 1.4	2.0 ± 0.2	0.44 ± 0.14	—	—	—	—	—	—	—	0.005
D-Ser-D-Abu	—	3.0 ± 0.7	3.5 ± 0.6	1.16 ± 0.3	—	—	—	—	—	—	—	—
D-Abu-D-Abu	NA	NA	0.05 ± 0.01	NA	—	—	—	—	—	—	—	—
D-Thr-D-Thr	NA	NA	0.1 ± 0.03	NA	—	—	—	—	—	—	—	—
ATP	3.6 ± 0.65	—	—	—	0.11 ± 0.02	—	—	—	1.9	—	—	—

^aData are from Refs. 21 and 32.

Interestingly, incubation of VanG in the presence of D-[1-¹⁴C]Ser and the same series of substrates showed that VanG was able to synthesize only a few D-Ser-D-X dipeptides, where X could be D-Ser, D-aminobutyrate, or D-norvaline (Fig. 2B). This result is in contrast with that obtained for VanC2 where no D-Ser-D-Ser activity was detected (32).

Enzyme Kinetic Characterization—Kinetic parameters of VanG were determined for a number of mixed dipeptides (Table 2). As expected, high catalytic efficiency was obtained for D-Ala-D-Ser formation, which was ~5-fold higher than for VanC2 (32) due to an eight times lower K_m value for D-Ser binding at subsite 2. As shown by TLC substrate specificity assay, VanG also bound D-Ser at subsite 1 and synthesized the dipeptide D-Ser-D-Ser with a relative efficiency similar to that for D-Ala-D-Ala. However, according to its K_m value, D-Ala is likely to be the substrate of choice for binding at subsite 1. In addition, when D-Ser binds at subsite 1, D-aminobutyrate binds with 5-fold higher affinity than D-Ser at subsite 2, and the catalytic efficiency of D-Ser-D-aminobutyrate is 4-fold higher than that of D-Ser-D-Ser (Table 2). D-Aminobutyrate and D-threonine, which are the best substrates of VanG for D-Ala-D-X formation, did not bind at subsite 1. This indicates that although subsite 2 could have a broad substrate specificity, subsite 1 remains highly selective, accommodating only D-Ala and D-Ser but repelling D-aminobutyrate and D-threonine, which have an additional methyl group in their side chains in comparison with D-Ala and D-Ser. VanA was also reported to display D-Ala:D-Ser ligase activity (23), and for comparison, we determined the kinetic parameters of VanA for D-Ala-D-Ala, D-Ala-D-Ser, and D-Ala-D-Lac formation (Table 2). Overall, the values obtained were similar to those reported previously (23). The K_m of VanG for D-Ser was 248-fold lower than that of VanA, leading to higher (>450-fold) catalytic efficiency. For D-Ala-D-Ala formation, the catalytic efficiency of VanG was only 6-fold higher. An additional difference between the two enzymes was the binding affinity for ATP, which, for VanG, was 33-fold lower than that for VanA, suggesting differences in the nucleotide binding sites.

Overall Structure of VanG—VanG crystallized with two independent molecules forming a homodimer in the asymmetric unit (Fig. 3A). Difference electron density maps revealed clear density for the polypeptide chains from residues 2–348 of both monomers, except for a gap from residues 89–92 near a pseudo two-fold axis of the dimer. Each monomer comprised three domains (Fig. 3B) as reported for VanA (14) and DdlB

(13). The N-terminal domain (residues 2–130) was formed by three α -helices and a core of seven β -sheets, whereas the central (residues 131–223) and C-terminal (residues 224–348) domains were formed by four α -helices and four and five β -strands, respectively. The nucleotide and substrate binding sites were located between the central and the C-terminal domains. Interactions in the dimer interface were both hydrophobic and electrostatic, with a buried surface area of 1790 Å² as calculated from the European Bioinformatics Institute (EBI) PISA web-based server (33). The overall structures of the two monomers of VanG were very similar except for the omega loop regions (residues 248–262), which differed significantly in conformation and orientation (Fig. 4A).

Superposition of the VanG monomer with that of VanA (PDB code: 1E4E) showed that the nucleotide and substrate binding sites were structurally homologous except for significant variations in the conformation and position of the omega loop and in the serine-serine 150S loop (Gly-188–Phe-191) (Fig. 3B). The major secondary and tertiary structural variations occurred in the central domain, mostly in the number and position of the α -helices (Fig. 3B).

Nucleotide Binding Site—As reported for other D-Ala:D-X ligases (13–15), the nucleotide binding site is formed by two antiparallel β -sheets from the central and C-terminal domains. The position and orientation of ADP in the binding site are highly conserved. Solvent accessibility calculations indicated that ADP is completely buried in the active site of the VanG ligase. The principal interactions involved in ADP binding are hydrophobic, ion pairs, and hydrogen bonds. The adenine ring of ADP is buried in a hydrophobic pocket formed by Phe-181, Ile-193, Ile-222, Phe-252, Tyr-258, and Phe-301. Access to the ADP binding site of monomer A in the dimer is partly blocked by residues from the omega loop of a symmetry-related molecule in the crystal (Fig. 4A). The nucleotide base of ADP makes a π - π stacking interaction with the aromatic side chain of Phe-181. The N6 atom of ADP forms hydrogen bonds with the side chain oxygen atom of Glu-219 and the carbonyl group of Glu-220, whereas the N1 and N7 atoms make hydrogen bonds with the main chain of Ile-222. In the ribose moiety, the O₂' atom forms a hydrogen bond with the side chain of Glu-226, and the O3' atom interacts with a water molecule in the binding pocket. The interaction established by the ribose differentiates VanG from other D-Ala:D-X ligase structures where O3' also interacts with Glu-226. The α - and β -phosphate atoms of ADP form

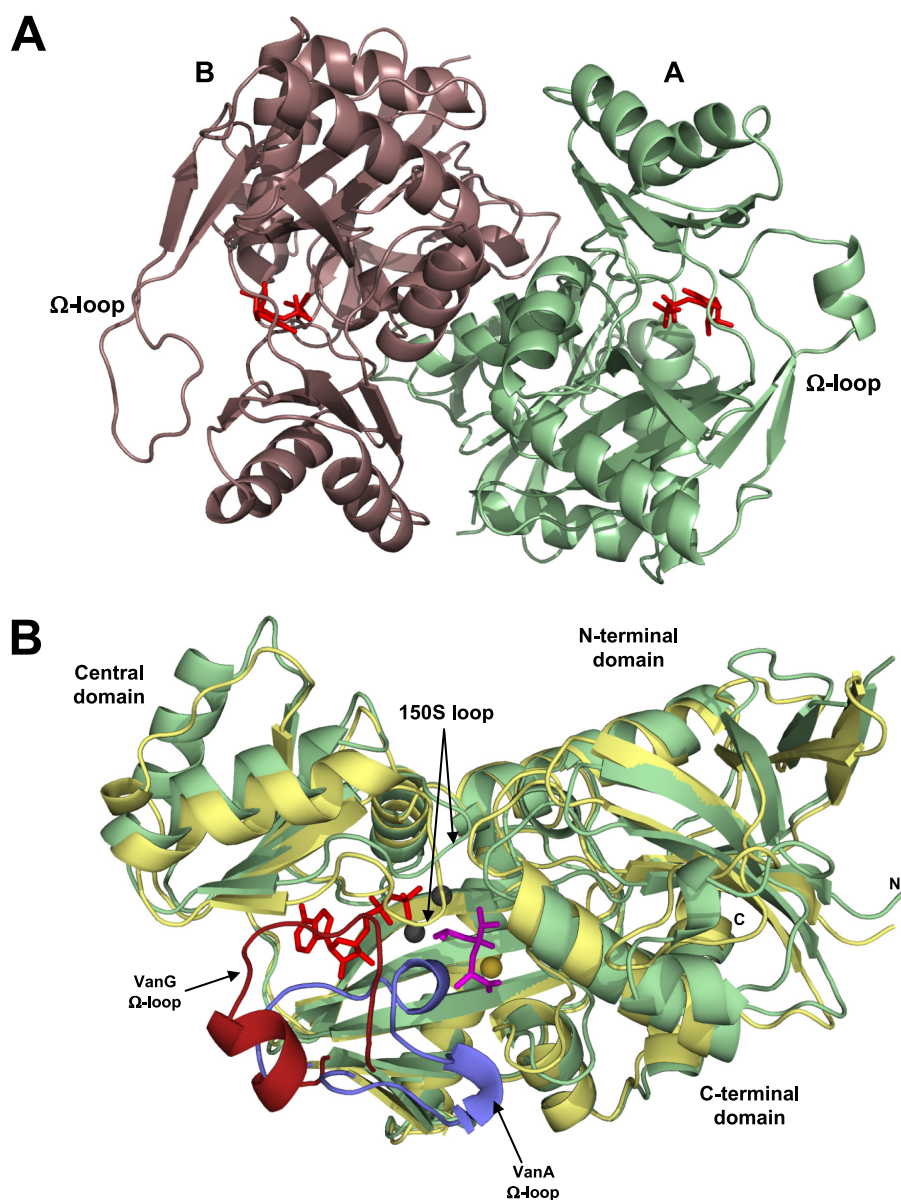


FIGURE 3. **Overall structure of VanG.** A, structure of the VanG homodimer. The omega loops of the two monomers have significantly different conformations. ADP is shown in red. B, VanG monomer A (green) superimposed on VanA (yellow) (PDB code 1E4E). The phosphophosphate inhibitor in the VanA structure is colored in magenta, and the magnesium ions are shown as gray spheres. A sulfate ion (yellow sphere) is located in the subsite 2 active site of VanG. The omega loops of VanG and VanA are colored in dark red and light blue, respectively. The serine-serine (150S) loops are indicated by arrows.

ion-pair interactions/hydrogen bonds with the side chains of Lys-140, Lys-183, Asn-311, and Glu-312. The β -phosphate atom also makes hydrogen bonds with Ser-190. This residue is part of the 150S loop that is present in all D-Ala:D-X ligases and is responsible for refolding of the active site during catalysis (13).

Ligand Binding Site—Our attempts to determine the structure of VanG in complex with the phosphinate analog of D-Ala-D-Ser by co-crystallization or by soaking were unsuccessful. This could be due to the presence of a bound sulfate ion (from the crystallization solution) in the ligand binding site near the position of the phosphinate analog described in other Ddl structures (Fig. 3B). Nevertheless, the structure of VanG reported here provides a description of the topology of the active site and insight into its molecular specificity. The resi-

dues present at subsite 1 are conserved and are in similar orientations as in VanA, in particular, the strictly conserved residues Glu-16, Val-19, and His-106 involved in D-Ala recognition (14). At subsite 2, the corresponding residues forming the oxyanion hole that interacts with the phosphinate analog are Arg-297, Asn-314, and Gly-318, but their position is shifted when compared with VanA (Fig. 5). However, a conformational shift upon substrate binding could bring these residues into proximity of the ligand. Based on interactions of the phosphinophosphate inhibitor in the active site of VanA, the carboxyl group of D-Ser in VanG could form hydrogen bonds with the side chain of conserved residue Ser-323 and with the amide group of Arg-324, and the hydroxyl group of D-Ser could be stabilized by the side chain of Arg-324, thus contributing to the specificity for serine at subsite 2 (Fig. 5).

Molecular Specificity of D-Ala:D-Ser Ligases

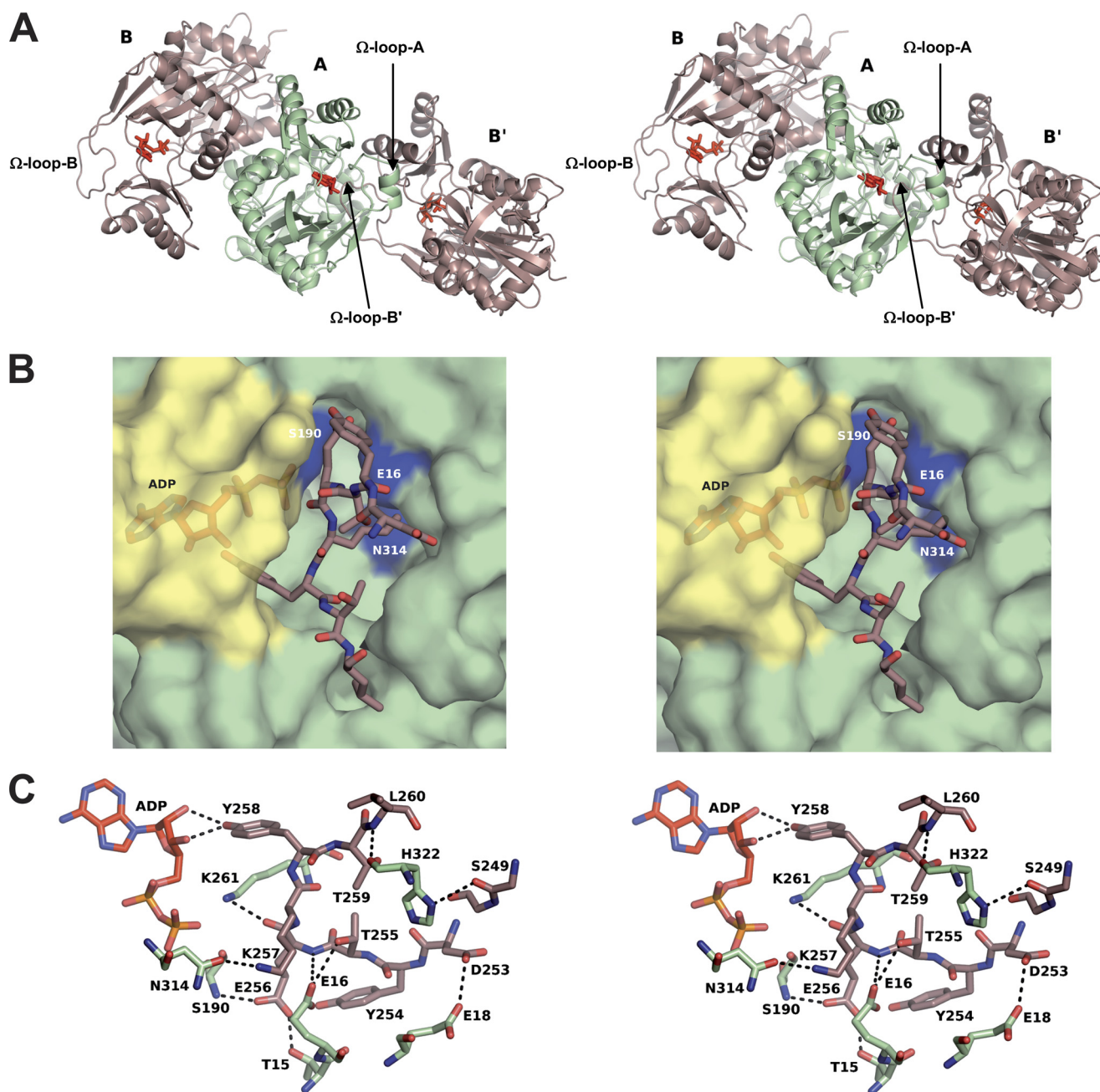


FIGURE 4. **Structural properties of the omega loop (stereo view).** *A*, interaction of monomer B' from a neighboring symmetry-related dimer (symmetry operation $-x - 1, -x + y - 1, -z + 1/3$) showing the omega loop deeply anchored in the active site of monomer A. *B*, contact surface area of the B' omega loop in the substrate binding site of monomer A. The conserved residues Glu-16, Ser-190, and Asn-318 of monomer A involved in substrate binding and catalysis in D-Ala:D-X ligases are shown in blue, and the omega loop of monomer A is in yellow. *C*, details of interactions involving residues of the omega loop of monomer B' (brown) with the substrate binding site residues of monomer A (green).

Structural and Functional Properties of the Omega Loop— Comparison of the two monomers of VanG revealed major structural differences in the omega loop region from residues 248–262, with differences of more than 12 Å in α -carbon positions at residues Tyr-258 and Thr-259 (Fig. 3A). The omega loop of monomer A of the dimer completely buries the ADP binding site, leaving partial access to the substrate binding site.

Monomer B' from a neighboring dimer makes extensive hydrophobic and electrostatic interactions with monomer A in the crystal, with a total buried surface area of 1359 Å² (Fig. 4A).

These interactions involve direct contacts of the omega loop with the ADP and substrate binding sites of an adjacent monomer A related by crystallographic symmetry (Fig. 4A). The interface contains a number of buried water molecules. Details of the electrostatic interactions in the binding interface are summarized in Table 3 and Fig. 4C. The buried surface of omega loop residues 248–262 in the interface is 814 Å². Residue Thr-255 of monomer B' makes a hydrogen bond with Glu-16 of the adjacent symmetry-related monomer A (Glu-16 participates in the binding of D-Ala at subsite 1 in other Ddl ligases) (Fig. 4, B and C). Glu-256 of the omega loop forms a

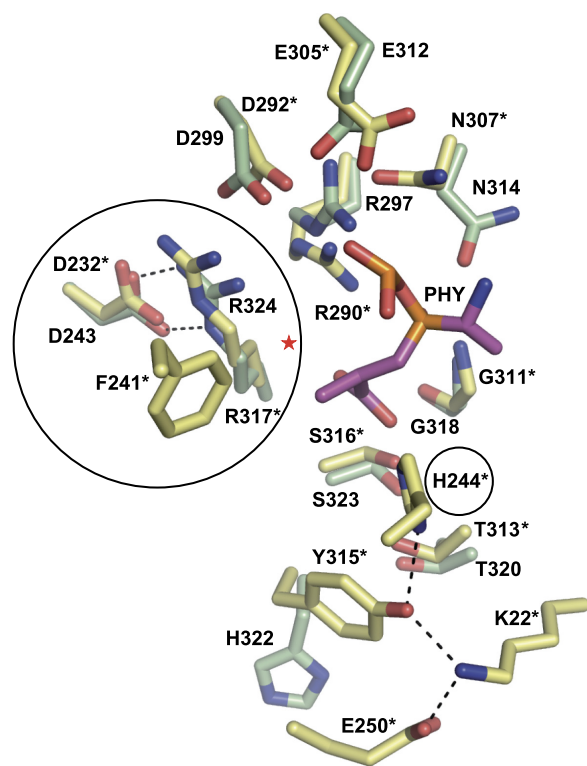


FIGURE 5. Active site residues of VanG (green) when compared with those of VanA (yellow) surrounding the phosphophosphinate inhibitor (PHY) modeled from VanA (PDB 1E4E) and LmDdl2 (PDB 1EHI) structures. The potential position of the D-Ser hydroxyl group is indicated by a red star. VanA residues are labeled with asterisks. The DFR triad involved in D-Ala-D-Ser specificity, common to VanG and VanA, is shown by the large circle. Residue His-244 of VanA, which is not present in VanG and is part of a hydrogen-bonding network, is indicated by a small circle.

TABLE 3
Major polar contacts between monomer A and the omega loop of monomer B' related by crystallographic symmetry

Monomer A (residue/atom)	Monomer B' (residue/atom)	Distance
Thr-15 OG1	Glu-256 OE1	2.48
Glu-16 ^a OE1	Thr-255 OG1	3.29
	Glu-256 N	3.46
Glu-16 ^a OE2	Glu-256 N	3.31
	Glu-256 OE1	3.18
Glu-18 OE2	Asp-253 OD2	3.01
Ser-190 ^a N	Glu-256 OE2	2.79
Lys-261 NZ	Glu-256 O	3.04
Asn-314 ^a OD1	Lys-257 NZ	2.98
His-322 ND1	Ser-249 O	3.48
His-322 O	Leu-260 N	2.88
ADP350 O3'	Tyr-258 OH	2.78
ADP350 O2'	Tyr-258 OH	3.09

^a Conserved residues among D-Ala:D-X ligases which are either involved in binding or catalysis.

hydrogen bond with Ser-190 in the 150S loop (important for substrate binding in other Ddl ligase structures) (Fig. 4, B and C). Lys-257 and Thr-258 of monomer B' are deeply buried in the binding interface and make hydrogen bonds with a sulfate ion and ADP, respectively, in the active site of the symmetry-related monomer A. In particular, Tyr-258 makes hydrogen bonds with the O2' and O3' atoms of the ribose moiety of ADP (Fig. 4C, Table 3).

Based on the unusual structural feature of the omega loop in the VanG crystal, we investigated the ability of an octapeptide,

Omega-1 (formyl-DYTEKYTL-NH₂), mimicking the omega loop sequence, to inhibit D-Ala:D-X ligase activity. Omega-1 was selected based on the contacts that the omega loop makes with the side chains of key active site residues involved in substrate binding or catalysis, *i.e.* Glu-16, Ser-190, and Asn-314 (Fig. 4C, Table 3). To ensure high similarity with the omega loop, Omega-1 was synthesized with C-amidated and N-formylated termini and was tested as a potential inhibitor of VanG, VanA, and StaDdl. Omega-1 was found to inhibit, in a dose-dependent manner, VanG and VanA but not StaDdl. At a 2 mM final concentration, the rates of inhibition were, respectively, 32, 58, and 9%, corresponding to IC₅₀ values of, respectively, 2.6 ± 0.06, 1.7 ± 0.06, and 11.2 ± 2.8 mM. As a control, two unrelated peptides of nine residues (RYYPYGSAL and GYNVTRYEV) were also tested and showed no inhibition at 5 mM final concentration, suggesting that inhibition by Omega-1 is specific.

DISCUSSION

Understanding the molecular basis of D-Ala:D-X ligase specificity is important for the development of antibiotics to overcome vancomycin resistance. The specificity of D-Ala:D-Lac ligases has been investigated by mutagenesis (21, 23, 34), three-dimensional structure determination (14, 16), and molecular docking of the LmDdl2 D-Ala:D-Lac ligase (35, 36). These studies provide evidence that the omega loop plays a central role in substrate selectivity at subsite 2. Selectivity of VanA for D-Lac was attributed to the positive charge of His-244, located in the omega loop, which could attract the negatively charged D-Lac substrate and reject the protonated form of the D-Ala amino group at the second subsite (14, 23), whereas in LmDdl2, Phe-261 could orient D-Lac favorably to achieve catalysis (36). The situation for D-Ala:D-Ser ligases is less clear. Based on the results of mutagenesis of VanA and VanC2 (21, 23), we have carried out the kinetic characterization and crystal structure determination of the VanG D-Ala:D-Ser ligase. This protein is phylogenetically close to the VanA D-Ala:D-Lac ligase (Fig. 1) despite the difference in resistance mechanisms mediated by these enzymes, an observation suggesting that they could share determinants for substrate specificity. However, kinetic analysis showed that VanG had high catalytic efficiency for D-Ala:D-Ser formation but no detectable depsipeptide ligase activity (Table 2).

The overall structure of VanG was found to be very similar to that of VanA, and the position of most active site residues was conserved in both nucleotide and ligand binding sites of the two enzymes (Figs. 3B and 5A). However, in the VanG ADP binding site, Glu-226 made a single hydrogen bond to the ribose moiety, whereas in VanA, both the O2' and the O3' atoms of the ribose ring established hydrogen bonds with the side chain of the structurally equivalent residue Glu-214. This difference may explain the lower affinity of VanG for ATP (Table 2). In addition, significant differences in the omega loop conformation were observed and could be due to the absence of the phosphophosphate inhibitor in the active site of VanG.

Interestingly, residues Arg-322 and Phe-250, which have a role in the D-Ser specificity of VanC2 (21), are also conserved in VanA (Arg-317 and Phe-241) and in VanG (Arg-324 and Phe-

Molecular Specificity of D-Ala:D-Ser Ligases

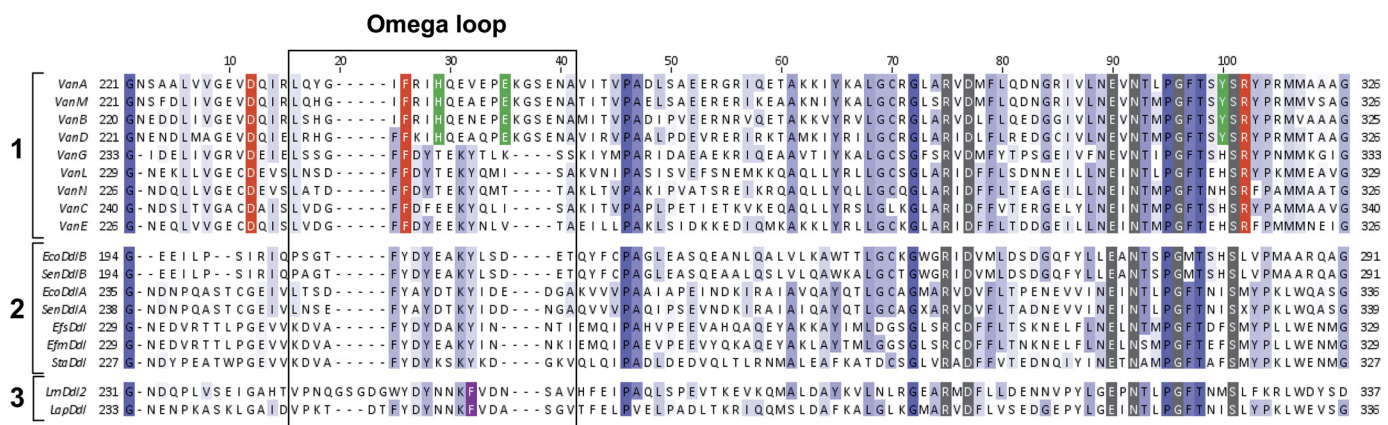


FIGURE 6. Alignment of the C-terminal domains of representative D-Ala:D-X ligases harboring the omega loop (box). Sequences are grouped as follows: group 1, VanA and VanC groups; group 2, D-Ala:D-Ala ligases; and group 3, D-Ala:D-Lac ligases from lactic bacteria. Conserved amino acids are highlighted in blue, and color intensity is dependent on the percentage of identity. Active site residues conserved in all D-Ala:D-X ligases are colored in gray. The residues of the DFR triad involved in D-Ala:D-Ser specificity are colored in red, and those stabilizing His-244 in VanA are shown in green. The phenylalanine determinant of D-Ala:D-Lac ligase in lactic bacteria is displayed in purple. Alignment was done by ClustalW (40), and the figure was generated using Jalview (41).

252) (Fig. 6). VanA was found to synthesize D-Ala-D-Ser, although with 450-fold lower catalytic efficiency than VanG (Table 2). This implies that His-244 in the omega loop would repel D-Ser from subsite 2, as it does for D-Ala, although the affinity for D-Ser was 4-fold higher than that for D-Ala (Table 2). Arg-317 (VanA) and Arg-324 (VanG) could make contact with the hydroxyl side chain of D-Ser and are stabilized by the acidic side chains of Asp-232 and Asp-243, respectively, indicating that the orientation of Arg-317 and Arg-324 is important for D-Ser specificity at subsite 2 (Fig. 5). Because mutation of the corresponding residue D241A in VanC2 results in a 14,000-fold decrease in D-Ala-D-Ser catalytic efficiency, whereas that of D-Ala-D-Ala formation is only 18-fold lower (23), this aspartate residue is also a specific determinant for D-Ala-D-Ser activity. The role of Phe-252 in VanG (Phe-250 in VanC2 and Phe-241 in VanA) is difficult to assess from the crystal structures. Phe-252 is located far from the active site in VanG due to the open folding form of the omega loop (Fig. 3A). However, in VanA, the main chain of the equivalent residue Phe-241 is within 4 Å from the methyl group of D-Ala and would be at an appropriate distance from the hydroxyl side chain of D-Ser (Fig. 5). Mutation F250Y in VanC2 leads to a 44-fold decrease in D-Ala-D-Ser catalytic efficiency (21). This residue probably plays a role similar to that of Phe-261 in LmDdl2 where the mutation F261Y resulted in complete loss of D-Ala-D-Lac activity (34). Recently, a molecular docking study showed that the F261Y mutation led to a nonproductive orientation of D-Lac (36). The corresponding residue Phe-252 in VanG is replaced by tyrosine in other D-Ala:D-Ala ligases (Fig. 6), suggesting that the active site of the vancomycin resistance enzymes (VanA and VanC groups) may have evolved to ensure a favorable orientation of D-Ser at subsite 2. Molecular docking studies are underway to test this hypothesis. Sequence alignment showed that residues Asp-243, Phe-252, and Arg-324 are strictly conserved in VanA and VanC groups but not in the other groups of D-Ala:D-X ligases (Fig. 6), indicating that this DFR triad is an important molecular signature for D-Ala-D-Ser specificity. Thus, enzymes of the VanA and VanC groups share determinants for D-Ala-D-Ser specificity, and both may have evolved from a common D-Ala:D-X ligase ancestor.

VanG was unable to synthesize D-Ala-D-Lac and D-Ala-D-hydroxyvalerate (Table 2), which is mainly due to the lack of the His-244 counterpart in the VanG omega loop. The sequence identity of VanG with the VanA group includes a number of residues (e.g. Lys-35, Ser-77, Asp-130, Phe-191, Glu-219, Asp-341...), which are distributed among all three structural domains and are thus unlikely to play a significant role in specificity. Although the omega loop containing His-244 appears to be a major determinant for D-Ala-D-Lac specificity, replacement of the VanC2 omega loop by that of VanA did not result in D-Ala-D-Lac or other depsipeptide synthesis (23). This indicates that other residues also play a role in specificity. In VanA, His-244 is part of a hydrogen-bond network involving Lys-22, Tyr-315, and Glu-250 (Fig. 5) (14), which are conserved in the VanA group; Tyr-315, which makes direct contact with His-244, is conserved only in the VanA group (Fig. 6). In VanG, the VanA Tyr-315 is replaced by His-322, which extends out of the active site cavity (Fig. 5). Thus, the Glu-250, Lys-22, Tyr-315, and His-244 hydrogen-bonding network is important for D-Lac recognition by assisting electron withdrawal from His-244 and appears to be a distinguishing feature of the VanA and VanC groups (Fig. 6). The evolutionary relationship between these two Van groups is of practical significance because these enzymes determine, in part, the resistance level of pathogenic bacteria to glycopeptides. Unlike the LmDdl2 ligase where the mutation F261Y switches synthesis of D-Ala-D-Lac to D-Ala-D-Ala (34), the evolution of ligase activity from D-Ala:D-Ser to D-Ala:D-Lac involves more than one or two residues because it includes the omega loop and at least Tyr-315. As reported for LmDdl2 (36), the switch of specificity and thus emergence of resistance could be due to an appropriate substrate orientation at subsite 2. The question then arises: could D-Ala:D-Ser ligases evolve to acquire depsipeptide ligase activity by selecting the hydroxyl group of D-Ser rather than the amino group for reaction with the alanylphosphate intermediate? This could generate a new mechanism for ligase activity conferring high levels of vancomycin resistance. It may be of interest to study the orientation of D-Ser and to see whether any mutations could favor ester over peptide bond formation.

Interaction of the omega loop with the active site of an adjacent monomer has not previously been described in other D-Ala:D-X ligase structures, and it is not known whether this intermolecular binding has any functional role. The extensive interactions and complementarity of the binding surfaces (Fig. 4) suggest using the omega loop sequence to select a potential peptide inhibitor for this family of enzymes. Glu-16, Ser-190, and Asn-314 of monomer A, strictly conserved residues involved in substrate binding or catalysis (13, 19), interact with the neighboring omega loop (Fig. 4, Table 3). The Omega-1 peptide inhibits VanG and VanA, but not StaDdl, suggesting a different mode of binding at the active sites of these enzymes. Omega-1 probably binds to the active site of VanG in the same manner as the omega loop in the crystal structure. However, it is difficult to predict the interaction geometry in VanA. Apart from the conserved active site residues involved in the interaction with the omega loop (Table 3), residues Thr-15, Glu-18, Lys-261, and His-322 in VanG have, respectively, Glu-15, Asp-18, Glu-250, and Tyr-315 as counterparts in VanA. In the case of StaDdl, the corresponding residues are Ala-15, Glu-18, Gly-255, and Phe-316. These differences could be responsible for the 2-fold difference in the inhibition rates of VanA and VanG and the very weak inhibition of StaDdl. To get more insight into the molecular recognition of Omega-1, we are currently trying to obtain the crystal structures of VanA and VanG in complex with the peptide inhibitor. Only a few peptide inhibitors of D-Ala:D-X ligases have been described (37), and all are analogs of the D-Ala-D-Ala product with K_i or IC_{50} values ranging from 0.5 to 6 mM. The IC_{50} values of Omega-1 for VanG and VanA were of the same order of magnitude. Thus, Omega-1 could provide a valuable model for the structure-based design of new D-Ala:D-X ligase inhibitors.

In conclusion, we report the first structure of a member of the vancomycin resistance D-Ala:D-Ser ligases and provide new insight into the molecular specificity and evolution of this family of enzymes. The structure of VanG reported here enabled us to describe a new peptide inhibitor and provided clues for the search for more effective peptide derivatives and for new antibiotics active against glycopeptide-resistant pathogens.

Acknowledgments—We acknowledge SOLEIL for provision of synchrotron facilities and thank the staff of beamline PROXIMA-1 for assistance. We thank C. T. Walsh (Harvard Medical School) for providing plasmid pIADLS4 and P. J. Stogios for critical reading of the manuscript.

REFERENCES

1. Arias, C. A., and Murray, B. E. (2012) The rise of the *Enterococcus*: beyond vancomycin resistance. *Nat. Rev. Microbiol.* **10**, 266–278
2. Reynolds, P. E. (1989) Structure, biochemistry, and mechanism of action of glycopeptide antibiotics. *Eur. J. Clin. Microbiol. Infect. Dis.* **8**, 943–950
3. Groves, P., Searle, M. S., Mackay, J. P., and Williams, D. H. (1994) The structure of an asymmetric dimer relevant to the mode of action of the glycopeptide antibiotics. *Structure* **2**, 747–754
4. Xu, X., Lin, D., Yan, G., Ye, X., Wu, S., Guo, Y., Zhu, D., Hu, F., Zhang, Y., Wang, F., Jacoby, G. A., and Wang, M. (2010) vanM, a new glycopeptide resistance gene cluster found in *Enterococcus faecium*. *Antimicrob. Agents Chemother.* **54**, 4643–4647
5. Lebreton, F., Depardieu, F., Bourdon, N., Fines-Guyon, M., Berger, P.,

6. Camiade, S., Leclercq, R., Courvalin, P., and Cattoir, V. (2011) D-Ala-D-Ser VanN-type transferable vancomycin resistance in *Enterococcus faecium*. *Antimicrob. Agents Chemother.* **55**, 4606–4612
7. Courvalin, P. (2006) Vancomycin resistance in Gram-positive cocci. *Clin. Infect. Dis.* **42**, S25–S34
8. Arthur, M., Molinas, C., Bugg, T. D., Wright, G. D., Walsh, C. T., and Courvalin, P. (1992) Evidence for *in vivo* incorporation of D-lactate into peptidoglycan precursors of vancomycin-resistant enterococci. *Antimicrob. Agents Chemother.* **36**, 867–869
9. Reynolds, P. E., Snaith, H. A., Maguire, A. J., Dutka-Malen, S., and Courvalin, P. (1994) Analysis of peptidoglycan precursors in vancomycin-resistant *Enterococcus gallinarum* BM4174. *Biochem. J.* **301**, 5–8
10. Arthur, M., Molinas, C., Depardieu, F., and Courvalin, P. (1993) Characterization of Tn1546, a Tn3-related transposon conferring glycopeptide resistance by synthesis of depsipeptide peptidoglycan precursors in *Enterococcus faecium* BM4147. *J. Bacteriol.* **175**, 117–127
11. Boyd, D. A., Willey, B. M., Fawcett, D., Gillani, N., and Mulvey, M. R. (2008) Molecular characterization of *Enterococcus faecalis* N06-0364 with low-level vancomycin resistance harboring a novel D-Ala-D-Ser gene cluster, *vanL*. *Antimicrob. Agents Chemother.* **52**, 2667–2672
12. Neuhaus, F. C. (1962) The enzymatic synthesis of D-alanyl-D-alanine. II. Kinetic studies on D-alanyl-D-alanine synthetase. *J. Biol. Chem.* **237**, 3128–3135
13. Mullins, L. S., Zawadzke, L. E., Walsh, C. T., and Raushel, F. M. (1990) Kinetic evidence for the formation of D-alanyl phosphate in the mechanism of D-alanyl-D-alanine ligase. *J. Biol. Chem.* **265**, 8993–8998
14. Fan, C., Moews, P. C., Walsh, C. T., and Knox, J. R. (1994) Vancomycin resistance: structure of D-alanine:D-alanine ligase at 2.3 Å resolution. *Science* **266**, 439–443
15. Roper, D. I., Huyton, T., Vagin, A., and Dodson, G. (2000) The molecular basis of vancomycin resistance in clinically relevant enterococci: crystal structure of D-alanyl-D-lactate ligase (VanA). *Proc. Natl. Acad. Sci. U.S.A.* **97**, 8921–8925
16. Liu, S., Chang, J. S., Herberg, J. T., Horng, M. M., Tomich, P. K., Lin, A. H., and Marotti, K. R. (2006) Allosteric inhibition of *Staphylococcus aureus* D-alanine:D-alanine ligase revealed by crystallographic studies. *Proc. Natl. Acad. Sci. U.S.A.* **103**, 15178–15183
17. Kuzin, A. P., Sun, T., Jorczak-Baillass, J., Healy, V. L., Walsh, C. T., and Knox, J. R. (2000) Enzymes of vancomycin resistance: the structure of D-alanine-D-lactate ligase of naturally resistant *Leuconostoc mesenteroides*. *Structure* **8**, 463–470
18. Kitamura, Y., Ebihara, A., Agari, Y., Shinkai, A., Hirotsu, K., and Kuramitsu, S. (2009) Structure of D-alanine-D-alanine ligase from *Thermus thermophilus* HB8: cumulative conformational change and enzyme-ligand interactions. *Acta Crystallogr. D Biol. Crystallogr.* **65**, 1098–1106
19. Wu, D., Zhang, L., Kong, Y., Du, J., Chen, S., Chen, J., Ding, J., Jiang, H., and Shen, X. (2008) Enzymatic characterization and crystal structure analysis of the D-alanine-D-alanine ligase from *Helicobacter pylori*. *Proteins* **72**, 1148–1160
20. Shi, Y., and Walsh, C. T. (1995) Active site mapping of *Escherichia coli* D-Ala-D-Ala ligase by structure-based mutagenesis. *Biochemistry* **34**, 2768–2776
21. Healy, V. L., Lessard, I. A., Roper, D. I., Knox, J. R., and Walsh, C. T. (2000) Vancomycin resistance in enterococci: reprogramming of the D-Ala-D-Ala ligases in bacterial peptidoglycan biosynthesis. *Chem. Biol.* **7**, R109–R119
22. Healy, V. L., Park, I. S., and Walsh, C. T. (1998) Active site mutants of the VanC2 D-alanyl-D-serine ligase, characteristic of one vancomycin-resistant bacterial phenotype, revert toward wild-type D-alanyl-D-alanine ligases. *Chem. Biol.* **5**, 197–207
23. Weber, P., Meziane-Cherif, D., Haouz, A., Saul, F. A., and Courvalin, P. (2009) Crystallization and preliminary X-ray analysis of a D-Ala:D-Ser ligase associated with VanG-type vancomycin resistance. *Acta Crystallogr. Sect. F Struct. Biol. Cryst. Commun.* **65**, 1024–1026
24. Lessard, I. A., Healy, V. L., Park, I. S., and Walsh, C. T. (1999) Determinants for differential effects on D-Ala-D-lactate versus D-Ala-D-Ala formation by the VanA ligase from vancomycin-resistant enterococci. *Biochemistry* **38**, 14006–14022

Molecular Specificity of D-Ala:D-Ser Ligases

24. Moubareck, C., Meziane-Cherif, D., Courvalin, P., and Périchon, B. (2009) VanA-type *Staphylococcus aureus* strain VRSA-7 is partially dependent on vancomycin for growth. *Antimicrob. Agents Chemother.* **53**, 3657–3663
25. Bugg, T. D., Dutka-Malen, S., Arthur, M., Courvalin, P., and Walsh, C. T. (1991) Identification of vancomycin resistance protein VanA as a D-alanine:D-alanine ligase of altered substrate specificity. *Biochemistry* **30**, 2017–2021
26. Daub, E., Zawadzke, L. E., Botstein, D., and Walsh, C. T. (1988) Isolation, cloning, and sequencing of the *Salmonella typhimurium ddlA* gene with purification and characterization of its product, D-alanine:D-alanine ligase (ADP forming). *Biochemistry* **27**, 3701–3708
27. McCoy, A. J., Grosse-Kunstleve, R. W., Adams, P. D., Winn, M. D., Storz, L. C., and Read, R. J. (2007) Phaser crystallographic software. *J. Appl. Crystallogr.* **40**, 658–674
28. Murshudov, G. N., Skubák, P., Lebedev, A. A., Pannu, N. S., Steiner, R. A., Nicholls, R. A., Winn, M. D., Long, F., and Vagin, A. A. (2011) REFMAC5 for the refinement of macromolecular crystal structures. *Acta Crystallogr. D Biol. Crystallogr.* **67**, 355–367
29. Collaborative. (1994) The CCP4 suite: programs for protein crystallography. *Acta Crystallogr. D Biol. Crystallogr.* **50**, 760–763
30. Emsley, P., and Cowtan, K. (2004) Coot: model-building tools for molecular graphics. *Acta Crystallogr. D Biol. Crystallogr.* **60**, 2126–2132
31. DeLano, W. L. (2010) *The PyMOL Molecular Graphics System*, version 1.3r1, Schrödinger, LLC, New York
32. Park, I. S., Lin, C. H., and Walsh, C. T. (1997) Bacterial resistance to vancomycin: overproduction, purification, and characterization of VanC2 from *Enterococcus casseliflavus* as a D-Ala-D-Ser ligase. *Proc. Natl. Acad. Sci. U.S.A.* **94**, 10040–10044
33. Krissinel, E., and Henrick, K. (2007) Inference of macromolecular assemblies from crystalline state. *J. Mol. Biol.* **372**, 774–797
34. Park, I. S., and Walsh, C. T. (1997) D-Alanyl-D-lactate and D-alanyl-D-alanine synthesis by D-alanyl-D-alanine ligase from vancomycin-resistant *Leuconostoc mesenteroides*: effects of a phenylalanine 261 to tyrosine mutation. *J. Biol. Chem.* **272**, 9210–9214
35. Neuhaus, F. C. (2010) Role of Arg301 in substrate orientation and catalysis in subsite 2 of D-alanine:D-alanine (D-lactate) ligase from *Leuconostoc mesenteroides*: a molecular docking study. *J. Mol. Graph. Model* **28**, 728–734
36. Neuhaus, F. C. (2011) Role of the omega loop in specificity determination in subsite 2 of the D-alanine:D-alanine (D-lactate) ligase from *Leuconostoc mesenteroides*: a molecular docking study. *J. Mol. Graph. Model* **30**, 31–37
37. Tytgat, I., Colacino, E., Tulkens, P. M., Poupert, J. H., Prévost, M., and Van Bambeke, F. (2009) DD-ligases as a potential target for antibiotics: past, present, and future. *Curr. Med. Chem.* **16**, 2566–2580
38. Saitou, N., and Nei, M. (1987) The neighbor-joining method: a new method for reconstructing phylogenetic trees. *Mol. Biol. Evol.* **4**, 406–425
39. Tamura, K., Peterson, D., Peterson, N., Stecher, G., Nei, M., and Kumar, S. (2011) MEGA5: molecular evolutionary genetics analysis using maximum likelihood, evolutionary distance, and maximum parsimony methods. *Mol. Biol. Evol.* **28**, 2731–2739
40. Chenna, R., Sugawara, H., Koike, T., Lopez, R., Gibson, T. J., Higgins, D. G., and Thompson, J. D. (2003) Multiple sequence alignment with the Clustal series of programs. *Nucleic Acids Res.* **31**, 3497–3500
41. Waterhouse, A. M., Procter, J. B., Martin, D. M., Clamp, M., and Barton, G. J. (2009) Jalview Version 2—a multiple sequence alignment editor and analysis workbench. *Bioinformatics* **25**, 1189–1191